Atmospheric
Chemistry
and Physics

Open Access

Discussions

Comparison of OMI UV observations with ground-based measurements at high northern latitudes

G. Bernhard[1], A. Arola[2], A. Dahlback[3], V. Fioletov[4], A. Heikkilä[2], B. Johnsen[5], T. Koskela[2], K. Lakkala[6], T. Svendby[7], and J. Tamminen[2]

[1]Biospherical Instruments, San Diego, California, USA
[2]Finnish Meteorological Institute, Helsinki, Finland
[3]Department of Physics, University of Oslo, Oslo, Norway
[4]Environment Canada, Toronto, Ontario, Canada
[5]Norwegian Radiation Protection Authority, Østerås, Norway
[6]Finnish Meteorological Institute, Arctic Research Centre, Sodankylä, Finland
[7]Norwegian Institute for Air Research, Kjeller, Norway

Discussion Paper | Discussion Paper | Discussion Paper | Discussion Paper

ACPD

15, 8933–8981, 2015

Comparison of OMI UV observations

G. Bernhard et al.

Title Page

Abstract	Introduction
Conclusions	References
Tables	Figures

|◀ | ▶|

◀ | ▶

Back | Close

Full Screen / Esc

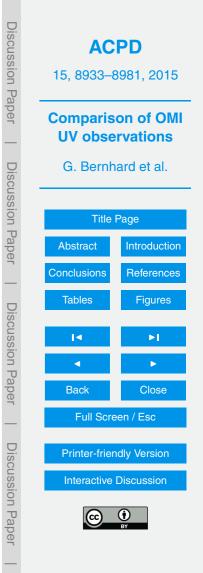Printer-friendly Version

Interactive Discussion

Abstract

The Dutch-Finnish Ozone Monitoring Instrument (OMI) on board NASA's Aura space-craft provides estimates of erythemal (sunburning) ultraviolet (UV) dose rates and ery-themal daily doses. These data were compared with ground-based measurements at 13 stations located throughout the Arctic and Scandinavia from 60 to 83° N. The study corroborates results from earlier work, but is based on a longer time series (eight vs. two years) and considers additional data products, such as the erythemal dose rate at the time of the satellite overpass. Furthermore, systematic errors in satellite UV data resulting from inaccuracies in the surface albedo climatology used in the OMI UV al-gorithm are systematically assessed. At times when the surface albedo is correctly known, OMI data typically exceed ground-based measurements by 0–11 %. When the OMI albedo climatology exceeds the actual albedo, OMI data may be biased high by as much as 55 %. In turn, when the OMI albedo climatology is too low, OMI data can be biased low by up to 59 %. Such large negative biases may occur when reflections from snow and ice, which increase downwelling UV irradiance, are misinterpreted as reflections from clouds, which decrease the UV flux at the surface. Results suggest that a better OMI albedo climatology would greatly improve the accuracy of OMI UV data products even if year-to-year differences of the actual albedo cannot be accounted for. A pathway for improving the OMI albedo climatology is discussed. Results also demonstrate that ground-based measurements from the center of Greenland, where high, homogenous surface albedo is observed year round, are ideally suited to de-tect systematic problems or temporal drifts in estimates of surface UV irradiance from space.

1 Introduction

The Dutch-Finnish Ozone Monitoring Instrument (OMI) on board the NASA EOS Aura spacecraft is a nadir viewing spectrometer that measures solar reflected and backscat-

tered radiation in a selected range of the ultraviolet and visible spectrum. The Finnish Meteorological Institute in collaboration with the NASA Goddard Space Flight Center have developed a surface ultraviolet irradiance algorithm for OMI that produces noon-time surface spectral UV irradia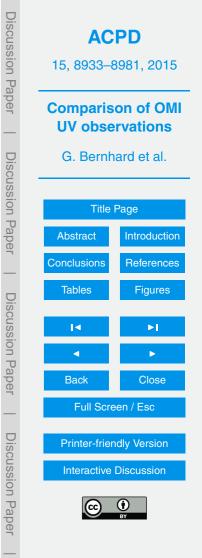nce estimates at four wavelengths, noontime erythemal dose rate or the UV index (UVI), and the erythemal daily dose. Tanskanen et al. (2007) (hereinafter referred to as T07) have compared erythemal daily doses derived from OMI observations with doses calculated from ground-based measurements of 18 reference instruments ranging in latitude from 72.6° N to 77.8° S. The present paper presents a similar comparison with focus on Arctic locations. Ground stations include 13 instruments located in Alaska, Canada, Greenland, Norway, Svalbard, and Finland (Fig. 1). These datasets are identical with those used by Bernhard et al. (2013), hereinafter referred to as B13.

Surface albedo from snow and ice covering the ground can enhance the clear-sky UVI by up to 58 % (Fig. 2). The effect is caused by photons that are reflected upward, and subsequently Rayleigh-scattered downward by the overlying atmosphere toward the surface (Lenoble, 1998). Fresh snow can have an albedo as high as 0.98 (Grenfell et al., 1994). Albedo decreases with snow depth but even a thin layer of fresh snow has a higher albedo than any other natural surface. According to Feister and Grewe (1995), the albedo of fresh snow at 310 nm is 0.62 for a snow depth of 2 cm and 0.76 for a depth of 5 cm. Calculations of the UVI from space-based measurements therefore require accurate knowledge of the surface albedo. Because OMI cannot distinguish between snow and clouds, an albedo climatology (Tanskanen, 2004) is used by the OMI UV algorithm. This climatology has unrealistic values at some locations and also does not take changes in albedo from year to year into account. According to T07, systematic errors in OMI UV data can be large (up 50 %) for polar regions because the OMI UV algorithm sometimes uses unrealistically small surface albedo that leads to misinterpretation of the observed bright scene as clouds. An important goal of the present paper is to quantify these systematic errors and their causes in greater detail, and to provide recommendations on how these errors could be reduced.

Comparison of OMI UV observations

G. Bernhard et al.

Title Page

Abstract	Introduction
Conclusions	References
Tables	Figures

◄ | ►|

◄ | ►

Back | Close

Full Screen / Esc

Printer-friendly Version

Interactive Discussion

T07 only considered daily erythemal doses. OMI data files also provide the UVI at the time of the satellite overpass and at local solar noon, and these data are also evaluated in the present paper. For estimating the daily dose, the OMI UV algorithm assumes that total ozone column (TOC) and cloud optical depth (COD) remain constant throughout the day, which is unrealistic in most cases. It may therefore be expected that differences between OMI and ground-based measurements assessed for the time of the satellite overpass are smaller than for the daily dose dataset. It is a secondary objective of the present paper to determine whether this is indeed the case.

The study by T07 is based on OMI data of the period September 2004–March 2006. The present study considers data measured between September 2004 and December 2012.

2 Datasets

The present paper focuses on the validation of the UVI and the daily erythemal dose. The UVI is a dimensionless number and calculated by weighting the spectral UV irradiance from Sun and sky that is received on a horizontal surface, $E_\lambda(\lambda)$, with the action spectrum for erythema, $s_{er}(\lambda)$, integrating the weighted spectrum over the wavelength range 250–400 nm, and multiplying the result by the constant k_{er}, which is equal to $40\,m^2\,W^{-1}$ (WHO, 2002):

$$\text{UVI} = k_{er} \times \int\limits_{250\,nm}^{400\,nm} E_\lambda(\lambda)s_{er}(\lambda)d\lambda = k_{er} \times E_{er},$$

where E_{er} is called the "erythemally weighted irradiance". Both ground-based and OMI data are based on the action spectrum for erythema defined by the Commission Internationale de l'Éclairage (CIE) in 1987 (McKinlay and Diffey, 1987). The spectrum has been slightly modified in 1998 (CIE, 1998; ISO, 1999). For solar zenith angles (SZAs)
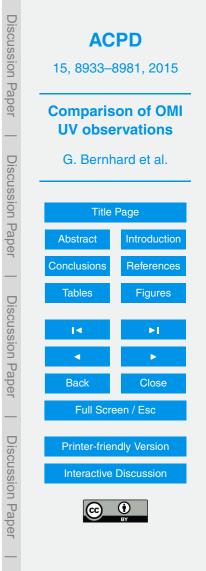
smaller than 60°, UVI values calculated with the new norm are approximately 0.5–1.0 % larger than corresponding values calculated with the original standard (Webb et al., 2011). Differences for SZAs between 60 and 90° are between 1–2 %. These differences should be taken into account when data of the present paper are compared with measurements that refer to the newer norm.

2.1 Ground based data

Ground-based data are identical with those used by B13 and are from thirteen Arctic and Scandinavian locations (Fig. 1). Sorted by decreasing latitude, the thirteen sites are Alert, Eureka, *Ny-Ålesund*, Resolute, Barrow, Summit, *Andøya*, Sodankylä, *Trondheim*, *Finse*, Jokioinen, *Østerås*, and *Blindern*. Sites that are italicized use multi-channel filter radiometers while the other sites use scanning spectroradiometers. Essential information such as the sites' latitude and longitude is provided in Table 1 of B13. Climatic conditions at the 13 sites are summarized by B13 and discussed in more detail in Sect. 5.1. Detailed information on instrumentation, data processing, and measurement uncertainties are also provided by B13. For all instruments but those installed at Sodankylä and Jokioinen, the expanded uncertainty (coverage factor $k = 2$) of UVI data ranges between 5.8 and 6.2 %. For the two Brewer spectrophotometers installed at Sodankylä and Jokioinen, a rigorous uncertainty budget has not been developed. However, the two instruments have participated in several intercomparision campaigns and were also regularly compared with the QASUME (Quality Assurance of Spectral UV Measurements in Europe) reference spectroradiometer (Bais et al., 2003). Measurements were consistently high by 1–6 % compared to measurements of the QASUME instrument. Data have not been adjusted to the irradiance scale of the QASUME instrument.

The erythemal daily dose was calculated by integrating measurements over 24 h periods, centered at local solar noon. Methods to fill data gaps have been described by B13.

2.2 OMI data

Details of the OMI surface UV algorithm have been discussed in detail by T07 and references therein. In brief, the algorithm first estimates the clear-sky surface irradiance using the OMI-measured total column ozo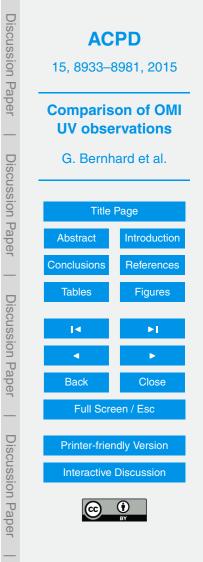ne, climatological surface albedo (Tanskanen et al., 2004), elevation, solar zenith angle (SZA), and latitude-dependent climatological ozone and temperature profiles. Next, the clear-sky irradiance is multiplied by a cloud modification factor (CMF) that accounts for the attenuation of UV radiation (UVR) by clouds and non-absorbing aerosols. The CMFs are derived from the measured reflectance at 360 nm, assuming that clouds are non-absorbing and their optical depth is independent of wavelength. Estimate of UVR are corrected for the effects of absorbing aerosols by applying a correction factor C_a as described by Arola et al. (2009). C_a typically ranges between 0.96 and 1.00 for the locations considered here.

OMI UV data were downloaded on 18 July 2014 from http://avdc.gsfc.nasa.gov/index.php?site=595385375&id=79. According to the file's header, the dataset is referenced as "EOS Aura OMI OMUVB (Collection 3, PGE v1.3; for ascending orbit only with SZA < 88)". These "overpass" data are provided by NASA's Aura Validation Data Center (AVDC) by filtering the Level 2 OMUVB data for over 250 ground stations where regular surface UV measurements are performed. Additional OMI UV products are available from the website http://omi.fmi.fi/products.html but these were not used for this study.

The OMI data files provide both E_{er} (in units of mW m^{-2}) and the UVI. Because the numerical precision of E_{er} is larger than that of the UVI (which is rounded to one decimal place), we used E_{er}, and divided the ground-based UVI measurements with k_{er} before comparing with the OMI data sets. The low precision of the native OMI UVI data is a particular problem for Arctic locations where the UVI is frequently smaller than 1.

The OMI overpass files contain several UV data products (Table 1). The data products (DP) assessed in the present paper include (1) the "Overpass Erythemal Dose

Rate"; the (2) "Erythemal Daily Dose Rate", (3) the "Clear Sky Erythemal Daily Dose Rate", (4) the "Erythemal Daily Dose"; and (5) the "Clear Sky Erythemal Daily Dose".

DP (1) is the erythemally weighted irradiance at the time of the satellite overpass. DP (2) is the erythemally weighted irradiance at local solar noon that is calculated from DP (1) by taking the difference of the SZA between the time of local solar noon and the time of the satellite overpass into account. The calculations assume that TOC and COD remain constant between the two times. DP (3) equals DP (2) without the CMF being applied. DP (4) is determined from the measured TOC and COD at the time of the overpass and the assumption that TOC and COD remain constant throughput the day. DP (5) equals DP (4) without the CMF being applied.
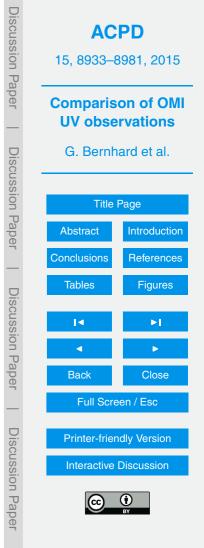
Data files contain additional information on data quality; SZA; viewing zenith angle (VZA); horizontal distance between the center of the OMI pixel (defined by the OMI Cross Track Position or CTP) and the nominal location (Dis); the value of the OMI surface albedo climatology used in the retrieval algorithm(SufAlbedo); Lambertian equivalent reflectivity (LambEquRef); terrain height (TerrHgt); and the COD estimated by the OMI UV algorithm (CldOpt). Some of these parameters were used for filtering the datasets when comparing with ground-based data. Because of the challenges to distinguish between high surface albedo and clouds from space, the method of selecting clear sky data by filtering for CldOpt = 0 may not be accurate.

At low latitudes, OMI measurements are nominally made once a day in the afternoon around 13:45 local solar time. At high latitudes, there is more than one satellite overpass per day. In these cases, the daily values of DPs (2)–(5) were averaged before comparing with ground-based data. When satellite data were filtered using some of the parameters mentioned above the number of data records contributing the daily average is reduced to one in most cases.

OMI overpass data files include data for Dis < 180 km. In particular for stations that are located close to the coast or situated on a mountain, the actual albedo as well as the albedo value SufAlbedo used in the OMI surface UV algorithm can change greatly over this distance. Figure 3 shows SufAlbedo for all ground station extracted

Comparison of OMI UV observations

G. Bernhard et al.

Title Page

Abstract	Introduction
Conclusions	References
Tables	Figures

|◄ | ►|

◄ | ►

Back | Close

Full Screen / Esc

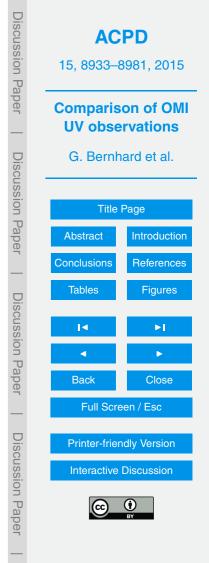Printer-friendly Version

Interactive Discussion

from the OMI data files. SufAlbedo is plotted for all data (black symbols) and data where Dis is either smaller than 12 km (blue symbols) or 5 km (red symbols). As can be seen from Fig. 3, values of SufAlbedo close to the station can differ substantially (e.g., by up to 0.65 during winter and spring at Finse and Ny-Ålesund) from values farther away. At Eureka, the albedo away from the station is biased high compared to values in close proximity. When the dataset is filtered for Dis < 12 km, values of SufAlbedo for a given day of the year are clustered to within ±0.05 for all sites but Finse. This site exhibits a bimodal distribution that even persist when the maximum distance is reduced to 5 km because adjacent pixels of the OMI albedo climatology have greatly different albedo values. For validating OMI, ideally only data should be used where the center of the OMI pixel is close to the ground station. However, by choosing a small value, the number of match-up data points is greatly reduced and the statistics of the comparison become less certain. Based on the results shown in Fig. 3, data were filtered for a maximum distance of 12 km, which we believe to be a good compromise.

3 Validation method

Ground-based data were linearly interpolated to either the time of the satellite overpass (DP (1)) or local solar noon (DP (2) and (3)). Daily dose data (DP (4) and (5)) did not require interpolation. Data were not used when the time between ground and satellite data was larger than the "maximum time" t_m. Sites that use multi-filter instruments typically provide a UVI measurement every minute and t_m for these sites was set to 5 min. Sites equipped with spectroradiometer provide measurements with a frequency ranging from 1 to 4 scans per hour. t_m was set to 30 min for Alert, Eureka, Resolute, Barrow, and Summit, and to 60 min for Sodankylä and Jokioinen.

To allow a comparison of results from this study to those by T07, similar metrics were used to quantify differences between the OMI and ground-based datasets. These are:

- $\rho_i = E_{s,i}/E_{g,i}$: ratio of satellite-derived data $E_{s,i}$ and ground based data $E_{g,i}$, where the index i indicates the data product (i = 1, 2, 3, 4, 5). Both $E_{s,i}$ and $E_{g,i}$ indicate "match-up" data for a particular record of the OMI data file. The quantity ρ_i defines a distribution, which in most cases cannot be well represented by a normal distribution. The statistics defined below were calculated both from monthly and annual distributions of ρ_i. These monthly and annual statistics include all years when data are available. It was further assumed that neither OMI nor ground-based data drift over time.

- N_i: the number of ρ_i contributing to the statistics of a given month or the year.

- $\overline{\rho}_i$: the average of ρ_i.

- $\widetilde{\rho}_i$: the median of ρ_i.

- Min_i and Max_i: the minimum and maximum values of ρ_i.

- $p_{f,i}$: the ratio at the fth-percentile with f = 5, 25, 75, and 95. For example, $p_{25,2}$ is the ratio at the 25th percentile of the ρ_2 distribution pertaining to DP (2). The difference between $p_{25,i}$ and $p_{75,i}$ is called the "interquartile range."

- $W_{10,i}$, $W_{20,i}$, $W_{30,i}$: percentage of satellite-derived data that agree to within 10, 20, and 30 %, respectively, with ground-based data.

As an alternative approach to quantifying the difference between OMI and ground data, we also calculated the monthly average from both datasets, and ratioed these averages:

$$R_i(y,m) \equiv \frac{\sum E_{s,i}(y,m)}{\sum E_{g,i}(y,m)},$$

where the summations are over all data within a given year y and month m, provided that both satellite and ground-based measurements are available. For each month,

Title Page

Abstract | Introduction

Conclusions | References

Tables | Figures

◄ | ►|

◄ | ►

Back | Close

Full Screen / Esc

Printer-friendly Version

Interactive Discussion

ratios $R_i(y, m)$ of all years were averaged and the resulting average is denoted $\overline{R}_i$. When at least 5 years of data were available, also the SD σ_i was calculated from the 5–9 annual values, allowing to quantify the variability of $R_i(y, m)$ from year to year. To avoid artifacts caused by data gaps when calculating monthly averages, only months with at least 20 days of data were considered. Despite this restriction, there could still be a bias in the monthly average if periods with missing days are not equally distributed in every year. For example, solar radiation tends to increase during months in the spring because the noontime SZA decreases. If measurements are missing at the beginning of a month, the monthly average will be biased high. To correct for this effect, the method developed by Bernhard (2011) was applied.
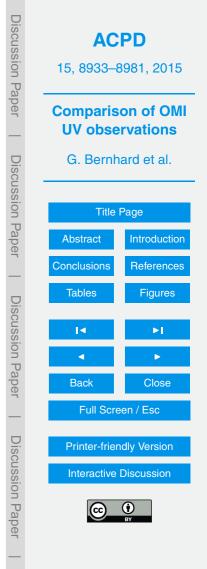
4 Results

As part of the analysis, the ratio and difference of OMI and ground UVI data were plotted for each site as functions of time, the UVI measured at the ground, and the day of the year. Furthermore, correlations between OMI and ground-based data were calculated and frequency distributions of OMI/Ground ratios were plotted for each month. This analysis was repeated for the five data products discussed in Sect. 3. The resulting wealth of information exceeds the space of this paper, however, the resulting plots and statistics are available as supplements: for each site and data product, a PDF page in a standardized format is provided. An annotated example of such a page is provided in Appendix A.

Because the values of ρ_i are not normal distributed and change greatly from month to month at some locations, box-whisker plots were chosen to visualize the results. Figure 4 shows these plots for DP (4). Data were filtered for SZA < 84° and Dis < 12 km. (The SZA was restricted to avoid that data affected by instrument noise skew the statistics. For SZA > 84°, the UVI is typically smaller than 0.2 and systematic errors at this low intensity are of little relevance.) Figure 4 indicates for each site and month the statistics $\overline{\rho}_4$, $\widetilde{\rho}_4$, $p_{5,4}$, $p_{25,4}$, $p_{75,4}$, and $p_{95,4}$. Statistics for the entire year are indicated
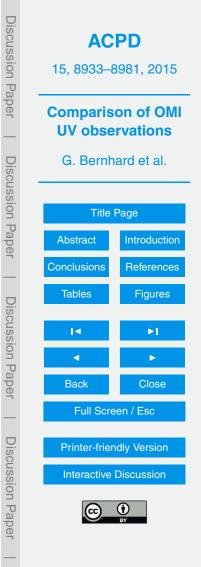
as the 13th month. Table 2 shows the comparison in tabular form. Two months were chosen for each site for this table: a month in spring when the surface is covered by snow and a month in summer when it is snow free. These months were selected based on the albedo climatology of Fig. 3. The OMI albedo climatology is invariant from year to year and therefore does not capture variability caused by the timing of snow melt. It can therefore be expected that ρ_i shows the highest variability in the "transition" months when snow melt occurs. On the other hand, for the "high winter" and "mid summer" months chosen for Table 2, a static albedo climatology is conceivably sufficient for accurate UVI retrievals from space-based observations.

Figure 4 and Table 2 indicate large systematic differences between OMI and ground data at some sites and for some months. For example, $\widetilde{\rho}_4$ is 0.60 between March and May at Ny-Ålesund, 1.55 in February and March at Trondheim, and smaller than 0.5 between January and April at Finse. On the other hand, the agreement between the two datasets is excellent at Summit and Sondakylä for all months. Good agreement is also observed during spring at Alert, Eureka, Resolute, and Barrow, and during summer at Ny-Ålesund, Finse, Jokioinen and Blindern. In Andøya and southern Scandinavian sites, the variability of the difference between OMI and ground daily doses is large as evidenced by the large interquartile range (e.g., Andøya in summer) and large whiskers (e.g., Blindern in autumn). The possible reasons for the observed systematic differences and variations between space- and ground-based observations are discussed in Sect. 5.

Figure 5 and Table 3 show box-whisker plots and validation statistics for overpass erythemal dose rate (DP (1)). These data were again filtered for SZA < 84° and Dis < 12 km. By comparing Fig. 4 with Fig. 5 and the values in Table 2 with those in Table 3, it can be seen that the distributions for DP (1) (as indicated by the interquartile range and the length of the whiskers) are generally much wider than those for DP (4) discussed earlier. This may be explained by the fact that ground measurements are a point measurement whereas OMI provides the mean surface UV over a large area (13 km × 24 km (along × across track) in nadir direction and increasing to

Comparison of OMI UV observations

G. Bernhard et al.

Title Page

Abstract | Introduction

Conclusions | References

Tables | Figures

|◄ | ►|

◄ | ►

Back | Close

Full Screen / Esc
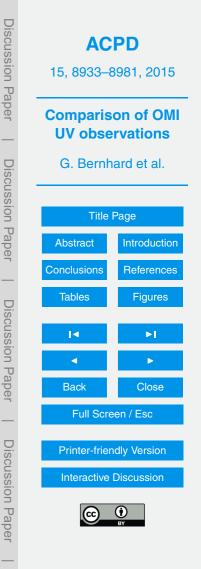
Printer-friendly Version

Interactive Discussion

13 km × 128 km at the most outer swath-angle of 57°, http://www.knmi.nl/omi/research/instrument/characteristics.php). The variability of the erythemal dose rate over the area of the OMI pixel is averaged in OMI data while ground measurement capture these fluctuations. Hence, the ratio of OMI/Ground is also affected by this variability, leading to the wide distributions evident in Fig. 5. The effect is largest at sites with high cloud variability and smallest at sites or seasons where clouds are either infrequent (e.g., Resolute in July) or where the attenuation of UVR by clouds is reduced by high surface albedo (e.g., Alert in spring, Summit all year). This reduction is the result of multiple scattering between the surface and cloud ceiling, which effectively traps light (e.g., Nichol et al., 2003).

As discussed in Sect. 1, the daily dose of ground measurements is calculated from the individual measurements performed throughout the day while the OMI UV algorithm assumes that the TOC and COD remain constant. The difference in sampling will result in variability in the ratio of the two datasets. The comparison of Fig. 4 with Fig. 5 suggest that the uncertainty of the OMI-derived erythemal daily dose introduced by the assumption of constant TOC and COD is smaller than the uncertainty in the OMI overpass erythemal dose rate applicable to a specific location, which is caused by the variability of this dose rate over the area of the OMI pixel.

The comparison of OMI and ground overpass erythemal dose rate data was repeated without filtering these data for SZA $< 84°$ and Dis < 12 km. As expected, distributions calculated without the filter were considerably larger than those obtained with the filter. These data are part of the Supplement.

Figure 6 is based on DP (4) and compares the average $\overline{\rho}_4$ and median $\widetilde{\rho}_4$ of the match-up statistics discussed earlier with the average ratio $\overline{R}_4$ derived from the monthly average daily doses. The median $\widetilde{\rho}_4$ agrees well with $\overline{R}_4$ for all sites and months, suggesting that biases between OMI and ground data assessed with match-up data (Fig. 4) are robust and also applicable to monthly doses. As explained in Sect. 3, the year-to-year variability of the OMI/Ground ratios is quantified with σ_4 and this SD is indicated by error bars in Fig. 6. At some sites (e.g., Summit, Sondankylä), the error

bars are smaller than the size of the symbol, highlighting that the bias between OMI and Ground data is nearly constant over time. At high-Arctic sites, σ_4 is typically small in March and April when the ground is covered by snow in all years. Similarly, σ_4 is small during summer at Scandinavian sites when the ground is snow free. As can be expected, σ_4 is largest in the transition months when the surface becomes snow free (e.g., June at Alert and Barrow, April at Finse) or when snow starts to accumulate again after the summer (e.g., September at Alert, October at Barrow).

All results presented above were based on the *ratio* of OMI and Ground data. For the large SZAs prevailing at high latitudes early in spring or late in fall, even large relative differences between the two datasets have only a small effect (with arguably negligible consequences) on absolute UVR levels. To emphasize this point, Fig. 7 shows box-whisker plots of the *difference* of OMI and Ground UVI measurements for the time of the satellite overpass. Statistics (i.e., whiskers, interquartile range, median, and average) were calculated the same way as for the analysis of ratios shown in Fig. 5. With few exceptions, the 25th and 75th percentile of the difference do not exceed ±1 UVI unit. Exceptions include June at Resolute (median bias of 1.0 UVI units), and April and May at Trondheim (bias of 1.2) and Finse (bias of −2.1).

5 Discussion

The effect of unrealistic albedo can either lead to a positive or negative bias of OMI UV data because the albedo is a key parameter when calculating the CMF. When the OMI parameter SufAlbedo exceeds the actual albedo ("Case 1"), the OMI UV algorithm interprets reflectance from clouds as reflectance from the surface and sets CldOpt to zero, resulting in CMF = 1. This has two effects, which both lead to a *positive* bias of OMI data. First, a high value of SufAlbedo leads to a high value of the derived clear-sky irradiance (e.g., Fig. 2). Second, since CMF = 1, the irradiance returned by the OMI UV algorithm is not reduced by cloud attenuation, in contrast to the irradiance seen by the instrument at the surface. High values of SufAlbedo lead to an inconsistency

when there are no clouds: in this case, the reflectance measured by the satellite is lower than that expected from the high value of SufAlbedo. This inconsistency could be exploited to improve the OMI albedo climatology. For example, data records with a large difference between the measured (low) reflectance and that expected from the high value of SufAlbedo could be selected for each grid point, and the albedo climatology could be adjusted until the difference disappears.

If SufAlbedo greatly underestimates the actual albedo ("Case 2"), reflectance from the surface is assumed to be caused by clouds, the cloud optical depth is set to a value larger than zero, resulting in CMF < 1. This has two effect, which both lead to a *negative* bias of OMI data. First, a low value of SufAlbedo leads to a low value of the derived clear-sky irradiance. Second, since CMF is smaller than 1, the irradiance returned by the OMI UV algorithm is further reduced. In contrast to Case 1, no inconsistencies can occur because high reflectance from snow measured during clear-skies can always (albeit incorrectly) be interpreted as cloud reflectance.

Examples of Cases 1 and 2 are provided in Sect. 5.1 when discussing results from the different sites.

It was anticipated that comparisons for overpass data show the least variability because this data product provides the best temporal match between satellite- and ground-based observations. Our results refute this hypothesis. The least variation was instead observed for the daily erythemal dose. The reason for this finding is likely due to ergodicity: for space-based observations, the variation introduced by clouds is spatially averaged over the area of the pixel while the temporal integration of ground-based measurements performed over the course of the day "smoothes" out cloud effects. The effects of spatial and temporal averaging seem to be similar.

5.1 Discussion by site

Results from each sites are briefly discussed below, with the exception of Summit and Barrow where more elaborate analyses are presented. Measurements from these two sites are completed with radiative transfer calculations, which are used for the inter-

Printer-friendly Version

Interactive Discussion

pretation of the difference of ground and satellite data. For Barrow, measurements of surface albedo and COD are also available and were used for interpretation. For other sites, the actual surface albedo was estimated from snow depth information. If not otherwise noted, systematic differences or "biases" discussed below refer to $\widetilde{\rho}_4$ and are expressed in percent (e.g., $\widetilde{\rho}_4 = 1.05$ corresponds to a bias of 5 %).

5.1.1 Alert, Canada

Alert is located close to the northernmost point of Canada. The bias for April and May (when SufAlbedo is about 0.8; Fig. 3) is less than 2 %. According to Canadian Climate Normals (CCN; http://climate.weather.gc.ca/climate_normals/) the ground at Alert is covered by more than 10 cm of snow at all days during these months. Results from Barrow (Sect. 5.1.6), which is an Arctic coastal site like Alert, indicate that an albedo of 0.8 is a reasonable value for these conditions. In June and July, the bias is about 15 %. SufAlbedo decreases from 0.75 to 0.25 during this period, which is likely too large considering that less than two days in July have a snow depth of 2 cm or larger. Variability of $\widetilde{\rho}_4$ is relatively high in the summer and fall when the surface is snow free. For example, the interquartile range is 0.99–1.05 in May, but 0.95–1.34 in July.

5.1.2 Eureka, Canada

Eureka is about 480 km southwest of Alert. OMI data are biased high by about 11 % between March and May when SufAlbedo is about 0.75. According to CCN, not all days during this period have snow cover in excess of 5 cm. The albedo value used by the OMI UV algorithm is therefore likely too large, which may explain the positive bias. The ground in July and August is virtually snow free (suggesting an albedo of less than 0.05, Blumthaler and Ambach, 1988) while SufAlbedo is between 0.1 and 0.2. Figure 2 suggest that up to 10 % of the of the bias of 12–19 % observed during these months could be caused by the relatively large values of SufAlbedo applied during these month.

5.1.3 Ny-Ålesund, Svalbard

Ny-Ålesund is at the west side of the Svalbard archipelago. Despite its high northern latitude, the climate is relatively mild because of the influence of the Gulf Stream. The bias at Ny-Ålesund between March and May is −40 %. SufAlbedo decreases from 0.35 to 0.20 during this period, which is likely far too low considering that snow cover at this time typically exceeds 50 cm. The underestimate is an example of the Case 2 mechanism discussed above. During July and August, when SufAlbedo is less than 0.15 and the ground is snow free, the bias is less than 6 %, confirming that OMI data are quite accurate when the albedo is accurately specified.

5.1.4 Resolute, Canada

Resolute is located about 600 km south of Eureka. Complete years of ground-based measurements at Resolute are only available in 2007, 2009, 2010, and 2011. Large data gaps at this site make statistics less robust (e.g., σ_4 could not be calculated for this site). In March and April, when SufAlbedo is 0.85 and snow cover exceeds 10 cm during more than 28 days per month according to CCN, the bias is 9 %, suggesting that the OMI albedo climatology is appropriate. On the other hand, there is a large bias of 48 % and large variability in June, when SufAlbedo drops from 0.85 to 0.5. CCN data indicate that snow disappears in June and the albedo values used by the OMI UV algorithm are therefore likely too large, explaining the large positive bias (Case 1).

5.1.5 Summit, Greenland

Summit is located near the top of the Greenland ice cap and has a very high surface albedo of about 0.97 year-round (Bernhard et al., 2008). Because of this high albedo, the influence of clouds is limited: the average attenuation of spectral irradiance at 345 nm is 3.5 % in spring and 5.8 % in summer (Bernhard et al., 2008). Because

of the small cloud effect and constant albedo, the scatter between OMI and ground observations is extremely small.

For sites located above 2500 m such as Summit, the OMI surface UV algorithm does not apply a cloud correction, i.e., clear-sky conditions are assumed for these altitudes at all times. This has to be taken into consideration when comparing OMI and ground data at Summit.

Figure 8a compares the medians $\widetilde{\rho}_1$, $\widetilde{\rho}_2$, and $\widetilde{\rho}_4$ of DP (1), DP (2), and DP (4), respectively. The median $\widetilde{\rho}_1$ for DP (1) (which was already shown in Fig. 5) is relatively constant and varies between 1.04 (equal to a bias of 4 %) in February and March and 1.10 (bias of 10 %) in August. The median $\widetilde{\rho}_2$ and $\widetilde{\rho}_4$ for DPs (2) and (4) exhibit an increasing tendencies with $\widetilde{\rho}_2$ ranging from 0.98 (bias of −2 %) in February to 1.14 (bias of 14 %) in August. The medians $\widetilde{\rho}_2$ and $\widetilde{\rho}_4$ are rather similar, except for February when $\widetilde{\rho}_4$ is 0.90.

Ground-based measurements at Summit are part of the Version 2 dataset of the NSF UV monitoring network (http://uv.biospherical.com/Version2/) referred to as "V2 dataset" in the following. This dataset includes clear-sky model data for every measurement. The availability of these model data presents the opportunity to better understand the reasons of the difference between OMI and ground-based measurements shown in Fig. 8a.

Model data were calculated with the radiative transfer model UVSPEC/libRadtran (Mayer and Kylling, 2005). Model input parameters are described in detail by Bernhard et al. (2008). In brief, parameters include: SZA; the extraterrestrial spectrum; atmospheric profiles of air density, temperature, ozone, and aerosol extinction; TOC; surface albedo; atmospheric pressure at station level; aerosol optical depth (τ_a); and single scattering albedo for aerosols. The TOC used for modeling was calculated from measured UV spectra according to the method by Bernhard et al. (2003). Surface albedo was set to 0.97 in accordance with measurements by Grenfell et al. (1994). The spectral dependence of τ_a was parameterized with Ångström's formula: $\tau_a = \beta\lambda^{-\alpha}$. Aerosol optical depth data for Summit are currently not available, and calculations

were performed for stratospheric background aerosol conditions by setting $\alpha = 1.0$ and $\beta = 0.008$. This translates to $\tau_a = 0.027$ at 300 nm. Actual values of τ_a are likely larger, in particular during spring when Summit may be affected by Arctic haze (VanCuren, 2012). Bernhard et al. (2008) suggest that aerosols may reduce spectral irradiance at 345 nm by about 1–3 % at Summit. Model data are therefore likely too large by this amount.
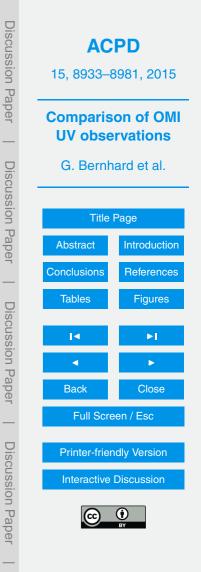
Figure 8b compares $\tilde{\rho}_1$ (solid red symbols) with the median calculated from the ratio of the model results and the ground based measurements (open red symbols). The two datasets agree to within ± 1.5 % for all months, but are biased high by 4–10 %. A bias of this magnitude is not surprising because neither the OMI UV algorithm nor the model take cloud attenuation into account. As mentioned earlier, cloud attenuate on average by 3.5 % between 1 March and 21 June and by 5.8 % between 22 June and 12 October (Bernhard et al., 2008).

Measurements performed during clear skies are flagged in the V2 dataset. Clear-sky periods are determined based on temporal variability of measured spectral irradiance at 600 nm as described by Bernhard et al. (2008). Ground-based, OMI, and model data were filtered for clear-sky periods, the comparisons between the three datasets were repeated, and results are indicated with blue symbols in Fig. 8b. The median ratio of OMI and ground overpass data (solid blue symbols in Fig. 8b) and the median ratios between model and ground data (open blue symbols) agree to within ± 3 %, but are both biased high by 2–6 %, depending on month. If measurements from ground and space as well as the model results were without error, the bias would be zero. The small bias that was actually observed is likely caused by a combination of several factors. First, attenuation by aerosols is not considered by either OMI or the model. Adjustment for this effect would reduce the bias by about 2–3 % in spring (when Arctic haze is potentially present) and 1 % in autumn. Second, the OMI albedo climatology for Summit is 0.9 in February and October, and 0.95 at the summer solstice. The albedo used by the model is 0.97 year round. Model results should therefore exceed OMI data by about 2 % most of the year. Third, ground-based data are traceable to the scale of

spectral irradiance established in 1990 by the US National Institute of Standards and Technology (NIST). The current (and presumably more accurate) NIST scale of 2000 is about 1.3 % higher in the UV-B than the 1990 scale (Yoon et al., 2002). If ground-based measurements were recalibrated to the NIST 2000 scale, the bias would be further reduced by about 1 %. Forth, the bias is within the expanded uncertainty of 6 % of the ground-based measurements (Bernhard et al., 2008) and some discrepancies can therefore be expected.

As noted earlier and illustrated in Fig. 8a, the bias for the erythemal daily dose rate (DPs (2)) and that of the daily dose (DP (4)), increase from about −1 % in March to 14 % in September. Several hypothesis were investigated and ultimately rejected to explain this increase. For example, the TOC is larger in spring than autumn. If the OMI algorithm used to convert the measurements at the time of the overpass to the time of local solar noon does not take the TOC correctly into account, this could conceivably result in a bias. When the ratio of EDRate/OPEDRate (see Table 1 for acronyms) was plotted vs. TOC, a strong correlation was indeed observed. However, when data were filtered by month, the correlation disappeared. For example, the ratio of EDRate/OPEDRate was similar for spring of 2010, when TOC was abnormally low, and spring of 2011, when it was abnormally high (B13). We therefore conclude that TOC cannot be the cause of the effect. Instead, the correlation with TOC only exists because TOC is effectively a proxy for time.

EDRate is calculated from OPEDRate by the OMI UV algorithm, taking into account the difference in SZA between the time of the overpass and the time of solar noon. Figure 9 shows the annual variation of EDRate/OPEDRate for Summit. (Additional analysis not shown here indicates a similar annual cycle of EDRate/OPEDRate for all sites.) The ratio increases with month, similar to $\widetilde{\rho}_2$ shown in Fig. 8a, but this change could be appropriate if the viewing geometry of OMI is different in spring and autumn. This is likely not the case, however. Figure 9 also indicates the time of the satellite overpass, illustrating that there is no difference between spring and autumn. Additional analyses also indicate that SZAs at the time of the overpass are not systematically

different in spring and autumn, and that the variation in the timing of local solar noon of about ± 15 min over the course of a year is too small to explain the effect. We conclude that the time-dependent bias in DP (2) shown in Fig. 8a is caused by a problem in the conversion from OPEDRate to EDRate applied by the OMI UV algorithm. Additional analysis suggests that the pa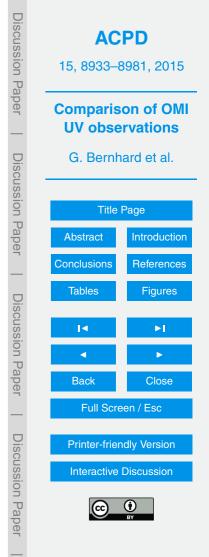ttern is likely due to a systematic error of up to ± 0.5° in the calculation of the local-noon SZA by the algorithm. For a SZA of 80° (local noon SZA on 1 March and 11 October at Summit), a 0.5° error in SZA results in a UVI error of about 8 %.

EDDose is calculated from EDRate by the OMI UV algorithm by applying a SZA-dependent function. The function was validated by calculating a corresponding ratio from the ground-based data. The result agreed with the function applied by OMI to within 2 %, except at SZAs exceeding 75°. At these large SZAs, the conversion function also becomes dependent on TOC, which is not taken into account by the OMI UV algorithm. This is the reason why $\widetilde{\rho}_2$ and $\widetilde{\rho}_4$ show a relatively large difference of 8 % for February in Fig. 8a while the difference is smaller than 2 % for the other months.

5.1.6 Barrow, Alaska

Barrow is close to the northernmost point of Alaska. The adjacent Chukchi Sea is typically covered by ice between November and July. Barrow is the only site considered here where the "effective surface albedo" (denoted a_{eff}) is routinely derived from ground-based measurements. a_{eff} is defined as the albedo of a uniform Lambertian surface, that, when used as input into a 1-D model, reproduces the measured spectrum (Lenoble et al., 2004). a_{eff} for Barrow is part of the V2 dataset and calculated from the spectral effect of surface albedo on the downwelling irradiance (Bernhard et al., 2006, 2007). The uncertainty (coverage factor $k = 1$) is 0.11 for $a_{\text{eff}} = 0.6$, and 0.09 for $a_{\text{eff}} = 0.85$. Figure 10 compares a_{eff} with SufAlbedo. Between March and mid-May, a_{eff} roughly varies between 0.70 and 1.00 while SufAlbedo is about 0.8. There is generally little bias between the two datasets. Snowmelt between mid-May and July leads to a sharp decrease of a_{eff}. While the general trend corresponds well with that of Su-

fAlbedo, there is a large variability, with a_{eff} sometimes being 0.4 smaller or larger than SufAlbedo. SufAlbedo starts to increase again at the beginning of September, while a_{eff} does not increase before October. Reliable snow coverage at Barrow was typically observed only after mid-October during the last decade (Bernhard, 2011). SufAlbedo in September and October is therefore likely too large by up to 0.3.

The bias of OMI daily dose data at Barrow is smaller than 9 % between February and April. The low value is consistent with the good agreement of a_{eff} and SufAlbedo in that period. While the bias for June is also small (−2 %), the scatter for this month is large (the interquartile range is 0.84 to 1.10), reflecting the larger inter-annual variability in a_{eff} for this month (e.g., Fig. 4). The bias for September and October is 38 and 62 %, respectively. This large positive bias can likely be explained by the Case 1 mechanism and is further investigated in the following.

Figure 11 compares the ratio EDRate/CSEDRate (which is equivalent to the CMF) with SufAlbedo and CldOpt for the year 2007. All data are from the OMI data file. Between mid-February and the end of April, CldOpt is zero with few exceptions, and the corresponding CMFs are one, as expected. Between June and September, CldOpt is frequently larger than 5, resulting in CMFs smaller than 0.7. In October, CldOpt is zero with few exceptions even though clouds remain frequent during this month. The low values of CldOpt are a consequence of the unrealistically large albedo for this month (Case 1).

Figure 12 shows statistics of cloud optical depth at Barrow from OMI (CldOpt) and ground-based observations. The box-whisker plot is based on data of all years, filtered for SZA < 84° and Dis < 12 km. Ground-based COD data are from the V2 dataset and were derived by comparing measurements of spectral irradiance at 450 nm with clear-sky model results (Supplement to Bernhard et al., 2004). To a good approximation (e.g., Fig. 5.16 of Liou, 2002), COD is independent of wavelength between 450 and 360 nm, the latter being the wavelength used by OMI to retrieve CldOpt.

COD of both datasets is close to zero for February, March, and April. There is also very good agreement between the two datasets for July, when the surface is snow free

and SufAlbedo is 0.03. Statistics of COD data from the V2 dataset for August through November are similar. In contrast, CldOpt is zero with few exceptions for October and November, confirming that the low CldOpt indicated in Fig. 11 for the year 2007 is the norm for these months. We conclude that the high bias of 62 % of OMI EDDose data for October is a consequence of the high value of the albedo climatology for this month, which in turn leads to an underestimate of the COD.
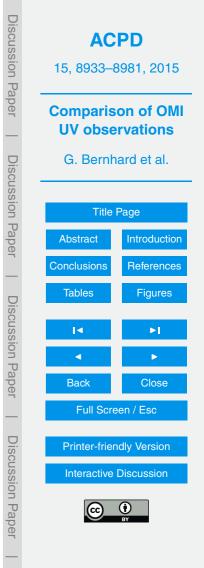
5.1.7 Andøya, Norway

Andøya is located on the Norwegian coast north of the Arctic Circle. The bias in March and April is less than ± 6 %; SufAlbedo is about 0.25. Winters are fairly mild due to the influence of the Gulf Stream and the relative low value of SufAlbedo is therefore reasonable. The bias for June through October is between 15 and 36 %, when SufAlbedo has an appropriate value of about 0.05. The relatively large bias can therefore not be explained by the OMI albedo climatology. When data are filtered for CldOpt = 0, the bias is reduced to 6–15 %. Hence, some portion of the bias is due to the cloud correction.

5.1.8 Sodankylä, Finland

The bias at Sodankylä between February and October ranges between 5 and 13 % and tends to be larger in winter/spring than summer. SufAlbedo is 0.5 between February and April, drops to 0.03 by the beginning of June, and remains below 0.03 for the remainder of the summer. Sodankylä is surrounded by boreal pine forests and peatlands for which an albedo of 0.03 in the erythemal band is appropriate (Blumthaler and Ambach, 1988; Feister and Grewe, 1995). Between June and August, a bias of 4–9 % is apparent in DP (1), (2) and (4), both for all data and data filtered for CldOpt = 0. The bias is therefore systematic and not related to potential errors in the CMF applied by the OMI UV algorithm. About half of the bias is within the uncertainty of the ground measurements.

5.1.9 Trondheim, Norway

Trondheim is located close to the coast of central Norway and has a predominantly hemiboreal oceanic climate. The bias is between 55 and 69 % between February and April. SufAlbedo for this period is 0.6. The albedo is likely too large considering that Trondheim is a city of 170.000 inhabitants and located on a fjord, about 50 km inland from the coast of central Norway. An albedo of 0.6 enhances the clear-sky surface UV dose only by 30 % (Fig. 2). A large part of the observed bias must therefore be caused by the Case 1 mechanism discussed earlier.

Of note, the bias for data filtered for CldOpt = 0 is very similar than that derived for all data, however, the large value of SufAlbedo affects the classification of cloud-free scenes. This is evident from the fact that also filtered data display a large day-to-day variability, which can only be explained by varying attenuation from clouds.

The bias between July and September is 14 % and SufAlbedo for this period is 0.04. The weather at Trondheim is predominantly cloudy also during summer. Because of the lack of clear-sky data, it is difficult to determine whether the bias is due to CMFs being too large or due to other causes.

5.1.10 Finse, Norway

The instrument at Finse is located on a mountain top, 1210 m a.s.l. and about 250 m above the tree line. The site is typically snow-covered between the months of September and June/July. Because of this location, surface conditions within the OMI pixel are generally different from those at the instrument site, and a large difference between satellite and ground observations can be expected. This is particular true for winter months when the immediate vicinity of the instrument is snow covered while the boreal forests within the OMI pixels are not. Indeed, the bias for February through May varies between −45 and −61 %. SufAlbedo has a bimodal distribution (either 0.55 or 0.70), which is likely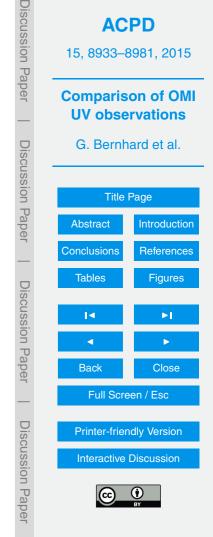 too low on many occasions. Between July and September, when the ground is snow-free, the bias is less than ± 3 %. This bias is smaller than for the

other Norwegian sites. One contributing factor for this relatively small bias is potentially the proximity of Finse to Hardangerjøkulen, a 78 km^2 large glacier located 5 km north of Finse. Because of the closeness to the glacier, the actual effective albedo for Finse during August could be larger than the surface albedo of 0.06 used by OMI, which would increase the ground measurement relative to the OMI observation and reduce the bias.

5.1.11 Jokioinen, Finland

Jokioinen is in the southwest of Finland, on the southern edge of the boreal forest belt, and has a temperate climate. Snow cover extends from December to March. The bias is −20 % between January and March, when SufAlbedo is 0.30. The actual albedo measured under overcast skies in February 2012 was 0.70 ± 0.08 (±1σ) according to Meinander et al. (2012). The negative bias is therefore likely caused by the Case 2 mechanism. Between April and November, the bias is less than ±6 % when SufAlbedo is 0.02. Hence, the albedo climatology used by OMI between April and December is almost ideal for this site and CMFs are calculated correctly.

5.1.12 Østerås and Blindern, Norway

Østerås and Blindern are suburbs of Oslo, about 6 km apart. Biases for both sites agree to within ± 2 % for all months except February and March when the bias at Østerås is 6 % smaller than at Blindern. Averaged over the year, the daily erythemal dose measured by OMI exceeds that measured at Østerås and Blindern by 7 and 8 %, respectively. SufAlbedo is about 0.15 between January and March and 0.02 between June and November, which are appropriate values. The influence of clouds at both sites is substantial and the observed biases suggest that the CMFs applied by the OMI UV algorithm are slightly too large.

5.2 Comparison with results by T07

Measurements at several sites discussed above (i.e., Eureka, Summit, Barrow, So-dankylä, and Jokioinen) have also been compared with OMI data by T07. Table 4 compares the medians $\widetilde{\rho}_4$ of these sites with those reported by T07. Results agree to within ±8 % with two exceptions: Barrow in March and Jokioinen in July. Differences of a few percent can be expected considering that the work by T07 is based on measurements performed between September 2004 and March 2006 only, while the present study uses data recorded between September 2004 and December 2012. In addition, values in Table 4 from the present study refer to months where the surface conditions are most certain (i.e., either snow covered or snow-free) while the classification of the surface condition applied by T07 is entirely based on the OMI albedo climatology: when albedo was higher than 0.1, snow cover was assumed, while the rest of the data were classified as snow-free. As discussed above (and also emphasized by T07), the true snow conditions may diverge from the OMI albedo climatology. For Barrow, $\widetilde{\rho}_4$ for March (when snow is present) is 0.99, while T07 reports a value of 1.20. The difference may be explained by the fact that the "snow cover" value by T07 also includes data from May, September and October, months where also the present study indicates large positive biases. For July at Jokioinen, $\widetilde{\rho}_4$ is 0.99 according to the present study; the corresponding value by T07 is 1.11. SufAlbedo for this month is 0.03, which should be an accurate value, supporting the smaller bias reported here.

6 Conclusions and outlook

UV data of the OMI instrument aboard NASA's Aura satellite were compared with measurements at 13 ground stations. OMI data files include several data products including the erythemal irradiance at the time of the satellite overpass, the erythemal irradiance at local solar noon, and the daily erythemal dose. The biases between OMI and ground-based instruments calculated for these data products are generally consistent,

Title Page

Abstract · Introduction

Conclusions · References

Tables · Figures

Back · Close

Full Screen / Esc

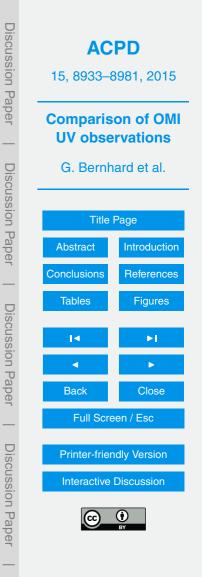Printer-friendly Version

Interactive Discussion

with few exceptions. For example at Summit, the bias between OMI and ground-based data evaluated at the time of the satellite overpass is almost constant throughout the year. In contrast, the biases for noon-time erythemal irradiance and the daily dose at this site increase from about −1 % in March to 14 % in November. This annual cycle was attributed to a problem in the OMI UV algorithm, specifically the calculation of the local-noon SZA. The problem also affect other sites to a similar degree.

At times when the surface albedo is known and correctly specified by the OMI albedo climatology, OMI data tend to exceed ground-based measurements by 0–11 %. Examples include Alert in April (OMI daily dose is biased high by 2 %), Ny-Ålesund in August (6 % bias), Barrow in July (10 % bias), and Østerås and Blindern year round (7 % bias). When the OMI albedo climatology exceeds the actual albedo, OMI data can be biased high by as much as 55 % (e.g, Trondheim in February and March). The bias is caused by two effects that go in the same direction: an unrealistically high value of the OMI albedo climatology leads to a high estimate of the clear sky irradiance and to an underestimate of attenuation by clouds. In turn, when the OMI albedo climatology is too low, OMI data can be biased low by as much as 59 % (e.g, Ny-Ålesund in March). Calculated biases are generally consistent with those published by T07 for those sites considered both by T07 and the present study. While relative difference can be large, absolute differences in terms of the UVI remain modest at all sites (e.g., the median bias is smaller than 2 UVI units at all sites; Fig. 7) because the large SZAs prevailing at high latitudes limit the UVI to less than 8 at all sites considered here. The relatively small UVIs observed in the Arctic and the resulting modest differences between OMI and Ground observations should not lead to the conclusions that UV radiation and its accurate measurement are not important. First, the day length in the Arctic can be as long as 24 h and organisms that cannot escape the Sun may be exposed to similar daily UV doses than those living at lower latitudes (Bernhard et al., 2010). Second, UV reflections from snow-covered surfaces can lead to considerable UV exposure to a person's face (Cockell et al., 2001), the eyes of an animal, and man-made materials used outdoors (Heikkilä, 2014).

A better albedo climatology could greatly improve the accuracy of OMI UV data products even if year-to-year differences in albedo are not accounted for. One way of improving the albedo climatology is to exploit an apparent inconsistency in OMI data: when the albedo climatology is too large, measurement of reflectance from space during clear skies can be lower than the reflectance that is expected from the (high) value of the albedo climatology. For locations and times where such an inconsistency is repeatably observed year after year, the climatological value could be reduced until the inconsistency disappears. The alternative is to combine measurements from OMI with data from satellites that are also sensitive in the IR or microwave region and which are able to distinguish reflectance from clouds and snow.

Due to rapidly changing albedo conditions, typically taking place during spring and autumn at high latitudes and mountainous regions, surface UV radiation products will always suffer from poorly known albedo unless real time data are available. Several satellite-based snow products have been developed recently for various applications. For example, the recently published global broad band albedo time series based on 5 day interval AVHRR data (Riihelä et al., 2013) could potentially improve the OMI albedo climatology. Such new albedo datasets should be considered when the next re-processing of OMI surface UV data will take place.

In order to improve the daily surface UV products targeted for the general public, an alternative solution would be to use daily snow information. For example, Aqua/MODIS snow products, which are observed close in time with OMI measurements, could be implemented.

Results presented in this study also showed that measurements at a high elevation site located at the center of a major ice sheet, such as Summit, are very helpful for satellite validation. Because of the high homogenous surface albedo at this site, cloud effects are suppressed, resulting in very small day-to-day variations when comparing data from space and the ground. Measurements at such a site are therefore ideally suited to detect systematic problems or drifts over time in the satellite dataset.

Comparison of OMI UV observations

G. Bernhard et al.

⊲ | ⊳

◄ | ►

Back | Close

Full Screen / Esc

Printer-friendly Version

Interactive Discussion

Appendix A: Standardized results plots

For each site and data product, a PDF page in a standardized format is available as Supplement to this paper. Figure 13 provides an annotated example of such a page. The page consists of five panels, labeled A–F. Panel A provides comparison statistics by months, specifically: N_i, Min_i, $p_{5,i}$, $p_{25,i}$, $\widetilde{\rho}_i$, $\overline{\rho}_i$, $p_{75,i}$, $p_{95,i}$, Max_i, $W_{10,i}$, $W_{20,i}$, and $W_{30,i}$. Panel B shows OMI and ground-based data plotted vs. time. Panel C is a scatter plot of OMI vs. ground data. Also indicated in panel C are results of two linear regressions to the data, one with the intercept calculated (red line) and one with the intercept forced through the origin (green). Dashed black lines indicate ±20 % deviations from the ideal 1 : 1 relationship (solid black line). Panel D consists of four sub-panels showing the *ratio* of OMI and ground data plotted vs. time, ground-based measurements, and day of the year, plus a box-whisker plot of the ratio statistics. Panel E provides similar plots for the *difference* of OMI and ground measurements. Panel F provides for every month a histogram of the frequency distribution of the OMI/Ground ratio. Note that the first plot of the sequence is the distribution for the whole year rather than January. The number of data points (N_i) that were used to calculate the distributions as well as $\widetilde{\rho}_i$ (green, labeled "Med") and $\overline{\rho}_i$ (red, labeled "Avg") are also indicated.

The Supplement related to this article is available online at doi:10.5194/acpd-15-8933-2015-supplement.
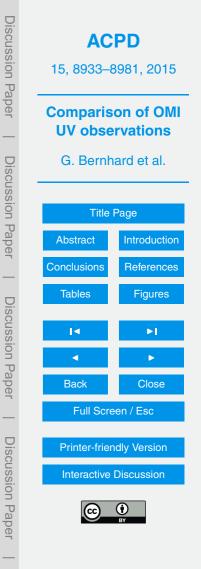
References

Arola, A., Kazadzis, S., Lindfors, A., Krotkov, N., Kujanpää, J., Tamminen, J., Bais, A., di Sarra, A., Villaplana, J. M., Brogniez, C., Siani, A. M., Janouch, M., Weihs, P., Webb, A., Koskela, T., Kouremeti, N., Meloni, D., Buchard, V., Auriol, F., Ialongo, I., Staneck, M., Simic, S., Smedley, A., and Kinne, S.: A new approach to correct for absorbing aerosols in OMI UV, Geophys. Res. Lett., 36, L22805, doi:10.1029/2009GL041137, 2009.

Bais, A., Blumthaler, M., Gröbner, J., Seckmeyer, G., Webb, A. R., Görts, P., Koskela, T., Rembges, D., Kazadzis, S., Schreder, J., Cotton, P., Kelly, P., Kouremeti, N., Rikkonen, K., Studemund, H., Tax, R., and Wuttke, S.: Quality assurance of spectral ultraviolet measurements in Europe through the development of a transportable unit (QASUME), in: Ultraviolet Ground- and Space-Based Measurements, Models, and Effects II, edited by: Gao, W., Herman, J. R., Shi, G., Shibasoki, K., and Slusser, J. R., SPIE, Bellingham, WA, USA, 4896, 232–238, 2003.

Bernhard, G.: Trends of solar ultraviolet irradiance at Barrow, Alaska, and the effect of measurement uncertainties on trend detection, Atmos. Chem. Phys., 11, 13029–13045, doi:10.5194/acp-11-13029-2011, 2011.

Bernhard, G., Booth, C. R., and McPeters, R. D.: Calculation of total column ozone from global UV spectra at high latitudes, J. Geophys. Res., 108, 4532, doi:10.1029/2003JD003450, 2003.

Bernhard, G., Booth, C. R., and Ehramjian, J. C.: Version 2 data of the National Science Foundation's Ultraviolet Radiation Monitoring Network: South Pole, J. Geophys. Res., 109, D21207, doi:10.1029/2004JD004937, 2004.

Bernhard, G., Booth, C. R., Ehramjian, J. C., and Nichol, S. E.: UV climatology at McMurdo Station, Antarctica, based on version 2 data of the National Science Foundation's Ultraviolet Radiation Monitoring Network, J. Geophys. Res., 111, D11201, doi:10.1029/2005JD005857, 2006.

Bernhard, G., Booth, C. R., Ehramjian, J. C., Stone, R., and Dutton, E. G.: Ultraviolet and visible radiation at Barrow, Alaska: climatology and influencing factors on the basis of version 2 National Science Foundation network data, J. Geophys. Res., 112, D09101, doi:10.1029/2006JD007865, 2007.

Bernhard, G., Booth, C. R., and Ehramjian, J. C.: Comparison of UV irradiance measurements at Summit, Greenland; Barrow, Alaska; and South Pole, Antarctica, Atmos. Chem. Phys., 8, 4799–4810, doi:10.5194/acp-8-4799-2008, 2008.

Bernhard, G., Booth, C. R., and Ehramjian, J. C.: Climatology of ultraviolet radiation at high latitudes derived from measurements of the National Science Foundation's Ultraviolet Spectral Irradiance Monitoring Network, in: UV Radiation in Global Climate Change: Measurements, Modeling and Effects on Ecosystems, edited by: Gao, W., Schmoldt, D. L., and Slusser, J. R., Tsinghua University Press, Beijing and Springer, New York, 544 pp., 2010.

Bernhard, G., Dahlback, A., Fioletov, V., Heikkilä, A., Johnsen, B., Koskela, T., Lakkala, K., and Svendby, T.: High levels of ultraviolet radiation observed by ground-based instruments below the 2011 Arctic ozone hole, Atmos. Chem. Phys., 13, 10573–10590, doi:10.5194/acp-13-10573-2013, 2013.

Blumthaler, M. and Ambach, W.: Solar UVB-albedo of various surfaces, Photochem. Photobiol., 48, 85–88, 1988.

Cockell, C. S., Scherer, K., Horneck, G., Rettberg, P., Facius, R., Gugg-Helminger, A., Driscoll, C., and Lee, P.: Exposure of Arctic field scientists to ultraviolet radiation evaluated using personal dosimeters, Photochem. Photobiol., 74, 570–578, 2001.

Commission Internationale de l'Éclairage (CIE): Erythema Reference Action Spectrum and Standard Erythema Dose, CIE S007E-1998, CIE Central Bureau, Vienna, Austria, 1998.

Feister, U. and Grewe, R.: Spectral albedo measurements in the UV and visible region over different types of surfaces, Photochem. Photobiol., 62, 736–744, 1995.

Grenfell, T. C., Warren, S. G., and Mullen, P. C.: Reflection of solar radiation by the Antarctic snow surface at ultraviolet, visible, and nearinfrared wavelengths, J. Geophys. Res., 99, 18669–18684, 1994.

Heikkilä, A.: Methods for assessing degrading effects of UV radiation on materials, Finnish Meteorological Institute Contributions No 111, Unigrafia. Oy., Helsinki, Finland, ISBN 978-951-697-843-0, 2014.

International Organization for Standardization/Commission Internationale de l'Eclairage (ISO/CIE): Erythema Reference Action Spectrum and Standard Erythema Dose. ISO 17166/CIE S007/E-1998, ISO, Geneva, Switzerland, 1999.

Lenoble, J.: Modeling of the influence of snow reflectance on ultraviolet irradiance for cloudless sky, Appl. Optimizat., 37, 2441–2447, 1998.

Lenoble, J., Kylling, A., and Smolskaia, I.: Impact of snow cover and topography on ultraviolet irradiance at the alpine station of Briançon, J. Geophys. Res., 109, D16209, doi:10.1029/2004JD004523, 2004.

Liou, K. N.: An Introduction to Atmospheric Radiation, Vol. 84, Academic Press, San Diego, California, 2002.

Mayer, B. and Kylling, A.: Technical note: The libRadtran software package for radiative transfer calculations – description and examples of use, Atmos. Chem. Phys., 5, 1855–1877, doi:10.5194/acp-5-1855-2005, 2005.

McKinlay, A. F. and Diffey, B. L.: A reference action spectrum for ultraviolet induced erythema in human skin, in: Commission International de l'Éclairage (CIE), Research Note, 6, No. 1, 17–22, 1987.

Meinander, O., Heikkilä, A., Riihelä, A., Aarva, A., Kontu, A., Kyrö, E., Lihavainen, H., Kivekäs, N., Virkkula, A., Järvinen, O., Svensson, J., and De Leeuw, G.: About seasonal Arctic snow UV albedo at Sodankylä and UV-VIS albedo changes induced by deposition of soot, in: Proceedings of Finnish Center of excellence in "Physics, Chemistry, Biology and Meteorology of Atmospheric Composition and Climate Change", and Nordic Center of excellence in Cryosphere-Atmosphere interactions in a changing Arctic climate, Annual Meetings 2012, Report Series in Aerosol Science, 134, 470–473, 2012.

Nichol, S. E, Pfister, G., Bodeker, G. E., McKenzie, R. L., Wood, S. W., and Bernhard, G.: Moderation of cloud reduction of UV in the Antarctic due to high surface albedo, J. Appl. Meteorol., 42, 1174–1183, 2003.

Riihelä, A., Manninen, T., Laine, V., Andersson, K., and Kaspar, F.: CLARA-SAL: a global 28 yr timeseries of Earth's black-sky surface albedo, Atmos. Chem. Phys., 13, 3743–3762, doi:10.5194/acp-13-3743-2013, 2013.

Tanskanen, A.: Lambertian surface albedo climatology at 360 nm from TOMS data using moving time-window technique, in: Ozone, Proceedings of the XX Quadrennial Ozone Symposium, 1–8 June 2004, Kos, Greece, edited by: Zerefos, C. S., Volume II, 1159–1160, published by University of Athens, Athens, Greece, 2004.

Tanskanen, A., Lindfors, A., Määttä, A., Krotkov, N., Herman, J., Kaurola, J., Koskela, T., Lakkala, K., Fioletov, V., Bernhard, G., McKenzie, R., Kondo, Y., O'Neill, M., Slaper, H., den Outer, P., Bais, A. F., and Tamminen, J.: Validation of daily erythemal doses from Ozone Monitoring Instrument with ground-based UV measurement data, J. Geophys. Res., 112, D24S44, doi:10.1029/2007JD008830, 2007.

Comparison of OMI UV observations

G. Bernhard et al.

Title Page

Abstract	Introduction
Conclusions	References
Tables	Figures

◄◄   ►►

◄   ►

Back   Close

Full Screen / Esc

Printer-friendly Version

Interactive Discussion

VanCuren, R. A., Cahill, T., Burkhart, J., Barnes, D., Zhao, Y., Perry, K., Cliff, S., and Mc-Connell, J.: Aerosols and their sources at Summit Greenland–first results of continuous size- and time-resolved sampling, Atmos. Environ., 52, 82–97, 2012.

Webb, A. R., Slaper, H., Koepke, P., and Schmalwieser, A. W.: Know your standard: clarifying the CIE erythema action spectrum, Photochem. Photobiol., 87, 483–486, 2011.

World Health Organization (WHO): Global Solar UV Index: a practical guide, 28 pp., published by World Health Organization (WHO), World Meteorological Organization (WMO), United Nations Environment Programme (UNEP) and the International Commission on Non-Ionizing Radiation Protection (ICNIRP), WHO, Geneva, Switzerland, available at: http://www.who.int/uv/publications/en/GlobalUVI.pdf (last access: 20 March 2015), 2002.

Yoon, H. W., Gibson, C. E., and Barnes P. Y.: Realization of the National Institute of Standards and Technology detector-based spectral irradiance scale, Appl. Optics., 41, 5879–5890, 2002.

Table 1. OMI data products assessed in the present paper.

Reference	Data product	Acronym	Unit
DP (1)	Overpass Erythemal Dose Rate (Satellite Measured Overpass UV Index)	OPEDRate OPUVindex	$\mathrm{mW\,m^{-2}}$ dimensionless
DP (2)	Erythemal Daily Dose Rate (Local Noon Time UV Index)	EDRate UVindex	$\mathrm{mW\,m^{-2}}$ dimensionless
DP (3)	Clear Sky Erythemal Daily Dose Rate (Local Noon Time Clear Sky UV Index)	CSEDRate CSUVindex	$\mathrm{mW\,m^{-2}}$ dimensionless
DP (4)	Erythemal Daily Dose	EDDose	$\mathrm{J\,m^{-2}}$
DP (5)	Clear Sky Erythemal Daily Dose	CSEDDose	$\mathrm{J\,m^{-2}}$

Data products in parenthesis were not directly assessed in the present paper because of their poor numerical precision compared to the corresponding erythemally weighted irradiance datasets. Data product names and acronyms are identical to those used in the OMI data files.

Table 2. Validation statistics[a] for daily erythemal dose (DP (4)).

Site	Month	Surface[b]	N_4	$\rho_{5.4}$	$\rho_{25.4}$	$\tilde{\rho}_4$	$\bar{\rho}_4$	$\rho_{75.4}$	$\rho_{95.4}$	$W_{10.4}$ [%]	$W_{20.4}$ [%]	$W_{30.4}$ [%]
Alert (82.50° N)	Apr	SC	74	0.93	0.98	1.02	1.04	1.11	1.17	73	96	99
	Jul	SF	97	0.67	0.95	1.14	1.17	1.34	1.78	31	47	65
Eureka (79.99° N)	Apr	SC	49	0.99	1.06	1.11	1.12	1.15	1.26	41	92	96
	Jul	SF	166	0.87	1.03	1.12	1.11	1.19	1.32	34	73	91
Ny-Ålesund (78.92° N)	Apr	SC	213	0.26	0.46	0.58	0.56	0.69	0.79	0	2	7
	Aug	SF	196	0.71	0.97	1.06	1.07	1.18	1.37	40	66	82
Resolute (74.72° N)	Apr	SC	72	0.95	1.05	1.09	1.08	1.11	1.22	58	92	99
	Aug	SF	96	0.74	1.20	1.24	1.25	1.33	1.63	7	16	63
Summit (72.58° N)	Mar	PSC	155	0.92	0.96	0.99	0.99	1.02	1.06	98	100	100
	Jul	PSC	128	1.06	1.08	1.11	1.11	1.14	1.19	44	96	100
Barrow (71.32° N)	Mar	SC	100	0.89	0.97	0.99	1.01	1.05	1.16	79	96	98
	Jul	SF	180	0.84	0.98	1.10	1.10	1.18	1.37	38	74	88
Andøya (69.28° N)	Mar	SC	186	0.67	0.87	0.96	0.97	1.03	1.28	48	72	83
	Aug	SF	175	0.84	1.07	1.17	1.29	1.41	2.01	26	51	61
Sodankylä (67.37° N)	Mar	SC	116	0.90	1.06	1.11	1.10	1.15	1.27	41	87	97
	Aug	SF	136	0.84	0.98	1.06	1.07	1.14	1.29	53	82	93
Trondheim (63.42° N)	Mar	SC	166	1.27	1.39	1.56	1.70	1.93	2.51	1	2	10
	Aug	SF	182	0.86	1.03	1.13	1.15	1.24	1.51	29	64	82
Finse (60.60° N)	Mar	SC	104	0.19	0.29	0.47	0.47	0.62	0.82	2	5	11
	Aug	SF	152	0.74	0.90	1.01	1.06	1.15	1.58	43	65	79
Jokioinen (60.82° N)	Feb	SC	125	0.54	0.67	0.79	0.80	0.87	1.24	10	29	50
	Jul	SF	164	0.78	0.92	0.99	1.00	1.07	1.22	53	84	93
Østerås (59.95° N)	Feb	SC	166	0.67	0.80	0.89	0.97	1.08	1.50	23	54	70
	Jul	SF	166	0.78	0.99	1.07	1.12	1.20	1.55	46	68	81
Blindern (59.94° N)	Feb	SC	160	0.72	0.84	0.94	1.06	1.12	1.91	26	57	75
	Jul	SF	163	0.82	1.01	1.07	1.10	1.17	1.50	48	72	86

[a] Match-up data were filtered for SZA < 84° and Dis; 12 km.
[b] SC = snow cover, SF = snow-free, PSC = permanent snow cover.

Table 3. Validation statistics[a] for overpass erythemal dose rate (DP (1)).

Site	Month	Surface[b]	N_1	$p_{5.1}$	$p_{25.1}$	$\tilde{\rho}_1$	$\bar{\rho}_1$	$p_{75.1}$	$p_{95.1}$	$W_{10.1}$ [%]	$W_{20.1}$ [%]	$W_{30.1}$ [%]
Alert (82.50° N)	Apr	SC	127	0.99	1.02	1.06	1.08	1.12	1.27	70	91	95
	Jul	SF	274	0.61	0.93	1.08	1.15	1.30	1.81	30	47	62
Eureka (79.99° N)	Apr	SC	68	1.07	1.11	1.14	1.15	1.17	1.27	18	84	97
	Jul	SF	293	0.89	1.01	1.10	1.10	1.16	1.34	41	83	91
Ny-Ålesund (78.92° N)	Apr	SC	494	0.28	0.49	0.60	0.61	0.73	0.90	4	11	19
	Aug	SF	467	0.75	0.92	1.05	1.10	1.23	1.65	36	60	75
Resolute (74.72° N)	Apr	SC	100	0.97	1.09	1.13	1.12	1.16	1.24	28	87	99
	Aug	SF	196	0.77	1.09	1.18	1.25	1.31	2.02	17	49	70
Summit (72.58° N)	Mar	PSC	320	0.98	1.02	1.05	1.05	1.08	1.15	84	98	100
	Jul	PSC	263	1.01	1.06	1.08	1.09	1.13	1.21	60	94	99
Barrow (71.32° N)	Mar	SC	166	1.00	1.05	1.09	1.10	1.14	1.27	59	90	96
	Jul	SF	277	0.82	0.97	1.08	1.11	1.17	1.53	40	71	84
Andøya (69.28° N)	Mar	SC	320	0.66	0.87	0.99	1.02	1.08	1.50	44	63	76
	Aug	SF	283	0.76	1.00	1.14	1.34	1.49	2.50	31	45	57
Sodankylä (67.37° N)	Mar	SC	187	0.93	1.07	1.13	1.14	1.18	1.45	32	79	89
	Aug	SF	214	0.84	0.97	1.05	1.16	1.18	1.82	51	73	84
Trondheim (63.42° N)	Mar	SC	208	1.23	1.38	1.59	1.91	1.94	3.84	0	3	11
	Aug	SF	229	0.85	1.03	1.11	1.24	1.31	2.03	34	62	72
Finse (60.60° N)	Mar	SC	115	0.16	0.27	0.47	0.48	0.62	0.91	4	8	12
	Aug	SF	204	0.66	0.85	1.01	1.27	1.37	2.49	28	40	54
Jokioinen (60.82° N)	Feb	SC	86	0.61	0.74	0.87	0.92	1.07	1.31	22	43	63
	Jul	SF	165	0.79	0.93	1.03	1.11	1.16	1.74	48	68	79
Østerås (59.95° N)	Feb	SC	209	0.66	0.81	0.92	1.03	1.09	1.87	28	56	75
	Jul	SF	211	0.78	0.98	1.08	1.33	1.38	2.57	40	57	66
Blindern (59.94° N)	Feb	SC	205	0.72	0.84	0.95	1.10	1.15	1.78	30	55	74
	Jul	SF	211	0.76	0.99	1.08	1.39	1.35	2.28	42	57	66

[a] Match-up data were filtered for SZA < 84° and Dis; 12 km.
[b] S = snow cover, SF = snow-free, PSC = permanent snow cover.

Table 4. Comparison of results from the present paper (PP) and those published by T07.

Site	Month	Surface[a]	$\widetilde{\rho}_4$ PP	T07[b]	Difference [%]
Eureka	Apr	SC	1.11	1.18	6
	Jul	SF	1.12	1.03	−8
Summit	Mar	PSC	0.99	1.06	7
	Jul	PSC	1.11	1.06	−5
Barrow	Mar	SC	0.99	1.20	21
	Jul	SF	1.1	1.18	7
Sodankylä	Mar	SC	1.11	1.10	−1
	Aug	SF	1.06	1.06	0
Jokioinen	Feb	SC	0.79	0.82	4
	Jul	SF	0.99	1.11	12

[a] SC = snow cover, SF = snow-free, PSC = permanent snow cover.
[b] Data are from Table 2 of T07.

Figure 1. Locations of instruments operated by Environment Canada (pink), Biospherical Instruments (blue), the Norwegian Radiation Protection Authority and the Norwegian Institute of Air Research (red), and the Finnish Meteorological Institute (black).

Figure 2. Enhancement of the clear-sky UVI as a function of albedo. The plot is based on radiative transfer calculations with the libRadtran model (Mayer and Kylling, 2005) for sea level, a TOC of 400 DU, and SZAs of 60°, 70° and 80° as indicated in the legend.

Figure 3. Surface albedo (SufAlbedo) of the OMI albedo climatology for each site, extracted from the OMI data files. Black symbols indicate all available data. Blue symbols indicate data where the distance (parameter "Dis") between the location of the stations and the center of the OMI pixel is smaller than 12 km. For red symbols, Dis is smaller than 5 km.

Comparison of OMI UV observations

G. Bernhard et al.

Figure 4. Ratio of the erythemal daily dose (DP (4)) measured by OMI and ground stations for each site. The box-whisker plots indicate for each month the 5th and 95th percentile (whisker), the interquartile range (box), median (line), and average (red dot). Statistics based on annual data are indicated as the 13th month. Match-up data were filtered for SZA < 84° and Dis < 12 km.
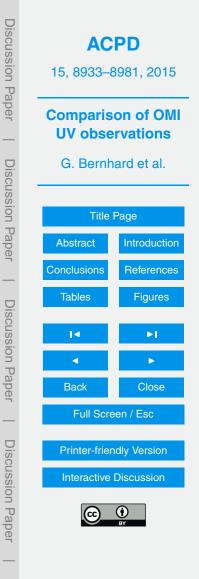
Figure 5. Same as Fig. 4 but for overpass erythemal dose rate (DP (1)).

Title Page

Abstract | Introduction

Conclusions | References

Tables | Figures

|◄ | ►|

◄ | ►

Back | Close

Full Screen / Esc
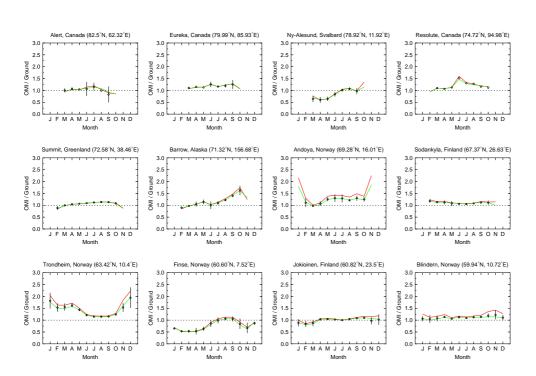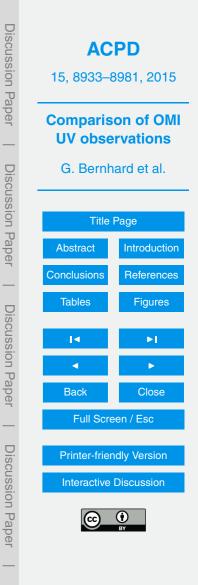
Printer-friendly Version

Interactive Discussion

Figure 6. Comparison of $\overline{\rho}_4$ (red lines), $\widetilde{\rho}_4$ (green lines), and $\overline{R}_4$ (open circles). The error bars indicate $\pm\sigma_4$. Data used for this figure were not filtered for SZA and Dis because such filtering would have reduced the number of data points of $\overline{R}_4$ substantially. Values of $\overline{\rho}_4$ and $\widetilde{\rho}_4$ are therefore slightly different from those indicated in Fig. 4.
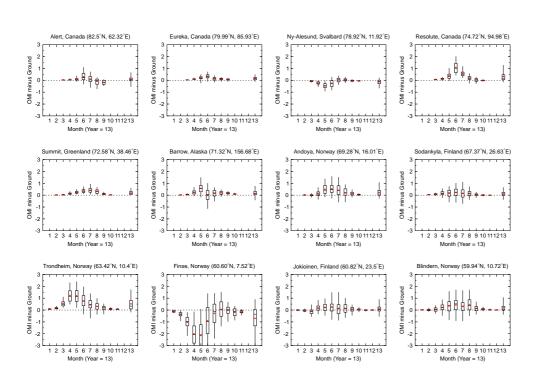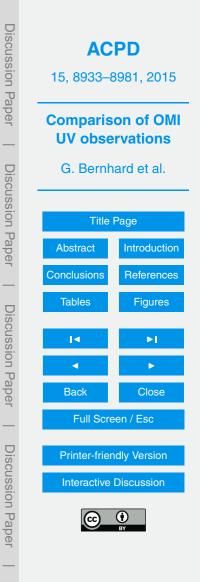
Figure 7. Difference of OMI and Ground UVI data, calculated from overpass erythemal dose rate data (DP (1)). The box-whisker plots indicate for each month the 5th and 95th percentile (whisker), the interquartile range (box), median (line), and average (red dot). Statistics based on annual data are indicated as the 13th month. Match-up data were filtered for SZA < 84° and Dis < 12 km.
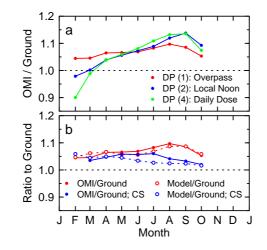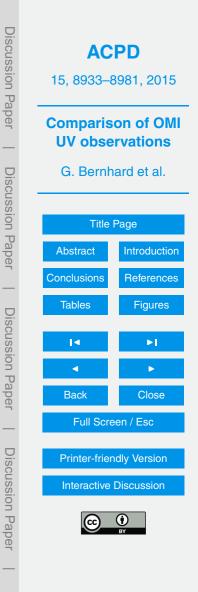
Figure 8. Comparison of OMI and Ground data at Summit. Panel **(a)**: median ratios $\tilde{\rho}_1$, $\tilde{\rho}_2$, and $\tilde{\rho}_4$ of DP (1), DP (2), and DP (4), respectively. Panel **(b)**: comparison of median ratios $\tilde{\rho}_1$ of OMI and Ground overpass measurements (solid symbols) with median ratios of modeled and measured data (open symbols). Results for data filtered for SZA < 84° and Dis; 12 km are indicated in red. Results for data that were additionally filtered for clear sky (CS) conditions are indicated in blue. The two datasets indicated by red solid symbols in Panels **(a)** and **(b)** are identical.
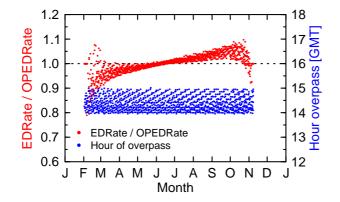
Figure 9. Ratio of EDRate/OPEDRate from OMI data file (red, left axis) and the hour of the OMI overpass (blue, right axis) derived from the Summit dataset. Data were filtered for VZA < 20°. The ticks on the x axis indicate the start of a given month.

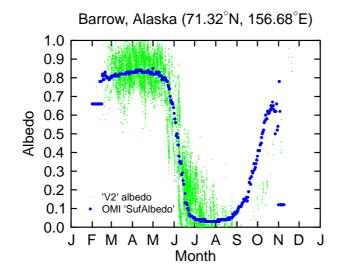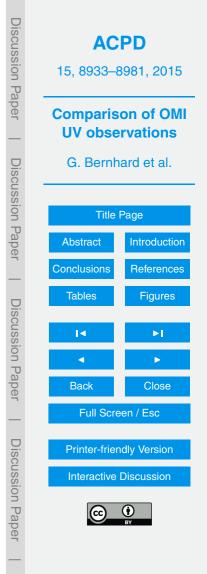**Figure 10.** Comparison of effective surface albedo a_{eff} derived from ground based measurements ("V2" albedo, green marker) with SufAlbedo (blue marker) of the OMI climatology for Dis < 12 km. a_{eff} data were measured between 1991 and 2013. a_{eff} data between September and November are sparse because of few clear-sky days during this period. The ticks on the x axis indicate the start of a given month.

Figure 11. Comparison of ratio EDRate/CDEDRate (grey, left axies), SufAlbedo (blue, left axis) and CldOpt (red, right axis). All data are from the OMI data file for Barrow and the year 2007. The ratio EDRate/CDEDRate is equivalent to the cloud modification factor (CMF).

Figure 12. Box-whisker plot of cloud optical depth retrieved from ground-based measurements (blue, left of month marker) and the corresponding CldOpt dataset from OMI (green, right of month marker) at Barrow. The averages for both datasets are indicated by red dots.

Barrow, Alaska (71.32°N, 156.68°E)
EDDose, SZA less than 84, Dist less than 12 km

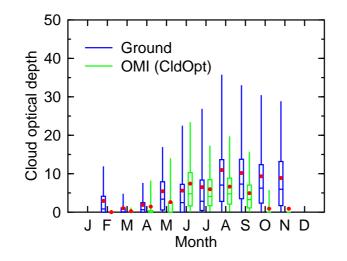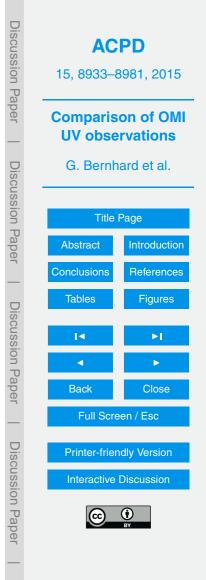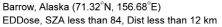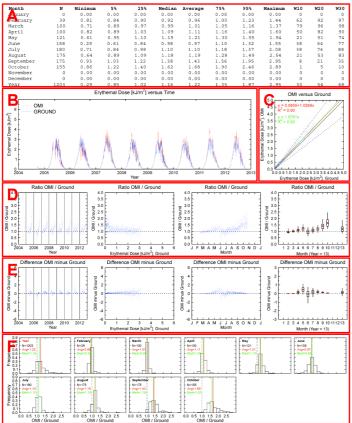| Month	N	Minimum	5%	25%	Median	Average	75%	95%	Maximum	W10	W20	W30
January	0	0.00	0.00	0.00	0.00	0.00	0.00	0.00	0.00	0	0	0
February	39	0.81	0.84	0.90	0.92	0.96	1.00	1.23	1.44	62	92	97
March	100	0.71	0.89	0.97	0.99	1.01	1.05	1.16	1.37	79	96	98
April	100	0.82	0.89	1.03	1.09	1.11	1.16	1.40	1.60	50	82	90
May	121	0.61	0.95	1.10	1.19	1.21	1.30	1.55	1.94	21	51	74
June	158	0.29	0.61	0.84	0.98	0.97	1.10	1.32	1.55	38	64	77
July	180	0.71	0.84	0.98	1.10	1.10	1.18	1.37	2.08	38	74	88
August	175	0.64	0.89	1.09	1.18	1.19	1.28	1.49	2.54	21	53	83
September	175	0.93	1.03	1.22	1.38	1.43	1.56	1.95	2.95	8	21	35
October	155	0.86	1.22	1.40	1.62	1.68	1.90	2.46	2.89	1	5	10
November	0	0.00	0.00	0.00	0.00	0.00	0.00	0.00	0.00	0	0	0
December	0	0.00	0.00	0.00	0.00	0.00	0.00	0.00	0.00	0	0	0
Year	1203	0.29	0.85	1.02	1.16	1.22	1.35	1.87	2.95	30	54	68

Figure 13. Example of a standardized page summarizing the results of the comparison of OMI and ground-based erythemal daily dose data at Barrow. Additional pages of this type are available as supplements. The contents of panels **(A–F)** are explained in the text.